Label-free characterization of peptide-lipid interactions using immobilized lipodisks

Víctor Agmo Hernández, Karin Reijmar and Katarina Edwards*

Department of Chemistry – BMC, Uppsala University, Box 579, SE-75123, Uppsala, Sweden

*victor.agmo@kemi.uu.se. Fax: +46 (0) 18 471 3654

Lipodisks, planar lipid bilayer structures stabilized by PEG-ylated lipids, were in the present study covalently bound and immobilized onto sensors for quartz crystal microbalance with dissipation monitoring (QCM-D) studies. It is shown that the modified sensors can be used to characterize the interaction of lipodisks with alpha-helical amphiphilic peptides with an accuracy similar to that obtained with well established fluorimetric approximations. The method presented has the great advantage that it can be used with peptides in their native form even if no fluorescent residues are present. The potential of the method is illustrated by determining the parameters describing the association of melittin, mastoparan X and mastoparan with immobilized lipodisks. Both thermodynamic and kinetic analyses are possible. The presented method constitutes a useful tool for fundamental studies of peptide-membrane interaction and can also be applied to optimize the design of lipodisks for, e.g., sustained release of antimicrobial peptides in therapeutic applications.

Introduction

Several reports in the literature have shown a wide range of applications of immobilized lipid structures, especially supported or tethered bilayer lipid membranes (sBLMs or tBLMs respectively) and adsorbed lipid monolayers. These systems can be used, e.g., as tools for the study of the properties of lipid membranes and how they are affected by the surrounding conditions (e.g., electric potential [1,2], composition of the bulk solution [3] etc.). They are also of great interest as systems to study membrane-analyte interactions, including the study of peptide- and protein-membrane interactions [4,5]. Furthermore, they can be used as supports for biologically relevant molecules, including membrane-bound receptors [6], in a biomimetic environment[7] or as supporting media for hydrophobic electroactive molecules [8-14] leading to the development of sensors. However, two major drawbacks can be readily identified in these systems. First, the total surface of available lipid membrane is given, and therefore limited, by the surface area of the substrate. Secondly, the presence of the support represents a difficulty when studying transmembrane proteins and it may also affect the intrinsic properties of the membrane[15]. Porous substrates and tBLMs (either to increase the surface area or to generate pore-spanning lipid bilayers) offer partial solutions to these problems, but they do not provide simultaneously with an increased available lipid surface area and with a membrane retaining its native properties. Recently, nanodiscs (nanoscale planar lipid bilayers stabilized by an amphiphatic protein belt) have been successfully immobilized on a wide range of sensor substrates[16-19], allowing for the study of membrane-analyte and membrane receptor-ligand interactions. However, the size of the nanodiscs is limited by the protein belt used and is usually in the range of 10-13 nm[20], implying that only a few hundred lipid molecules are found in each nanodisc. Related structures that can provide with much larger membrane surfaces are lipodisks, i.e., planar lipid bilayer structures whose rim is stabilized by polyethyleneglycol (PEG) modified lipids. In this report, the use of immobilized lipodisks is

proposed as a protein free alternative to nanodiscs capable of providing with a large lipid surface area while retaining the native properties of the lipid membrane. These disks are spontaneously formed when the appropriate proportions of lipids and PEG-ylated lipids are mixed together and suspended in water[21-23]. As both faces of the lipid bilayer are exposed to the surrounding media, lipodisks are ideal systems for interaction studies. Recent research has also shown that they are potentially useful as drug carriers[24]. Following adequate protocols, lipodisks can be immobilized on a variety of substrates, including quartz crystal microbalance (QCM)[5] and surface plasmon resonance (SPR)[25] sensors , as well as on chromatographic media[5,26,27]. This allows performing studies of, e.g., protein-membrane interactions[5,25] and drug partition[26].

In this report, a reproducible and robust protocol for the covalent binding of lipodisks to sensors for QCM with dissipation monitoring (QCM-D) experiments is presented. The obtained immmobilized lipodisks are employed to study and characterize their interaction with alpha-helical peptides. These peptides are of great interest in pharmaceutical applications, as some of them have antimicrobial activity. It has been shown that incorporation of these peptides into lipodisks is an excellent way of achieving a sustained release of the compound as well as to protect the peptide from enzymatic degradation [24]. The method described in this report is able to quantify the amount of peptide that can be carried by a lipodisk, as well as the physicochemical parameters describing the peptide-lipodisk association.

Experimental section

Chemicals

Dry powder of 1,2-di-palmitoyl-*sn*-glycero-3-phosphocoline (DPPC), 1-palmitoyl-2-oleoyl-*sn*-glycero-3-phosphocoline (POPC), 1-palmitoyl-2-oleoyl-*sn*-glycero-3-phosphoglycerol (POPG), 1,2-distearoyl-*sn*-glycero-3-phosphoethanolamine-N-(polyethylene glycol)-2000

(DSPE-PEG_{2000}), and 1,2-distearoyl-*sn*-glycero-3-phosphoethanolamine-N-[amino(polyethylene glycol)-2000] (DSPE-PEG_{2000}amine) were purchased from Avanti Polar Lipids (Alabaster, USA). 1,6-diphenyl-1,3,5-hextatriene (DPH), 11-mercaptoundecanoic acid (MUA), N-hydroxysuccinimide (NHS), N-(3-dimethylaminopropyl)-N'-ethylcarbodiimide hydrochloride (EDC), ethanolamine, sulfuric acid, hydrogen peroxide, sodium phosphate (mono- and di-basic), sodium chloride, octaethylene glycol monododecyl ether ($C_{12}E_8$), 5(6)-carboxyfluorescein (CF) mixed isomers and melittin (GIGAVLKVLTTGLPALISWIKRKRQQ) were purchased from Sigma Aldrich (Schnelldorf, Germany). Mastoparan (INLKALAALAKKIL) and mastoparan X (INWKGIAAMAKKLL) were products from BioNordika (Stockholm, Sweden). All aqueous solutions were prepared using deionized water (18.4 MΩ cm) obtained from a Milli-Q system (Millipore, Bedford, USA). QCM-D gold sensors were obtained from Q-Sense (Gothenburg, Sweden).

Lipodisk preparation

Extruded lipodisks consisting of a 75:21:4 mol/mol mixture of DPPC: DSPE-PEG_{2000}: DSPE-PEG_{2000}amine were prepared as follows. The lipids were weighted in a test tube in the desired proportions and dissolved in chloroform. The solvent was then removed under a flow of nitrogen until a film was formed on the tube walls. To ensure complete removal of the solvent, the sample was left overnight in a vacuum. The films thus prepared were either used immediately or stored at -20 ˚C in a nitrogen atmosphere. To prepare the lipodisks, the films were hydrated with phosphate buffer saline (PBS, 10 mM phosphate, 150 mM NaCl, pH = 7.4) at 55 ˚C for 30 min with intermitent vortexing. The sample was then subjected to 8 freeze-thaw cycles (freezing in liquid nitrogen and thawing at 55 ˚C) and, finally, extruded 15 times through a polycarbonate filter with a pore size of 100 nm (Avestin, Ottawa, Canada) using a Mini-Extruder (Avanti Polar Lipids, Alabaster, AL).

Fluorescence measurements

Peptide binding to the disks was determined using fluorimetric determinations for melittin and mastoparan X, both of which have a fluorescent tryptophan residue. The emission spectrum of this aminoacid is dependent on the polarity of its surroundings. The spectrum of a free tryptophan-containing peptide in water is red shifted compared to when it is associated to the lipid membrane. This shift can be used to determine the proportions of bound and free peptide, thus providing the data to construct an association isotherm that describes the peptide-lipodisk affinity[28]. A SPEX Fluorolog 1650 0.22-m double spectrometer (SPEX Industries, Edison, NJ) was used in the binding assay. All measurements were performed at 25°C. An aqueous solution of the studied peptide was loaded into a quartz cuvette and titrated with small additions from a lipodisks dispersion. Emission spectra at an excitation wavelength of 280 nm were acquired after each addition. The ratio between the emission fluorescence intensities at 325 and 355 nm (α) is directly related to the fraction of peptide associated to the lipodisks. The value of α is in all cases corrected for inner filter effects. α was determined as a function of the peptide to lipid mixing ratio, R_i. From these values, the effective associated peptide to lipid ratio (R_{eff}) at different values of R_i can be calculated from:

$$(\alpha \times R_i)/((1-\alpha)\times[P]_{tot,aq}) = R_{eff}/[P]_{aq} \qquad (1)$$

where $[P]_{tot,aq}$ is the total peptide concentration and $[P]_{aq}$ is the amount of peptide in the water phase.

QCM-D measurements

The immobilization of lipodisks and their interaction with alpha-helical peptides were followed using a Quartz Crystal Microbalance with Dissipation monitoring (QCM-D). A QCM-D E1 (Q-Sense, Gothenburg, Sweden) instrument thermostated at 21°C and with a controlled sample flow of 150 μL min^{-1} was employed for all experiments. Frequency and dissipation data was collected from the fundamental sensor frequency (5 MHz) as well as the

3rd, 5th, 7th, 9th, 11th and 13th overtones. Quantitative determinations of the immobilized mass were based on the model proposed by Voinova et al.[29] for the formation of viscoelastic films on QCM-D sensors. The model states that the overtone dependent shifts on oscillation frequency (Δf) and dissipation factor (ΔD) are dependent on the viscoelastic properties of the formed film. In the case of thin adsorbed films in a bulk liquid, the changes in frequency and dissipation are given by equations 2a and 2b:

$$\Delta f = -\frac{m_d n f_0}{t_q \rho_q} + \frac{4\pi^2 h_1 \eta_w \rho_w \eta_1 \left(n f_0\right)^3}{t_q \rho_q \left(\mu_1^2 + 4\pi^2 \eta_1^2 \left(n f_0\right)^2\right)} \tag{2a}$$

$$\Delta D = \frac{4\pi h_1 \eta_w \rho_w \mu_1 n f_0}{t_q \rho_q \left(\mu_1^2 + 4\pi^2 \eta_1^2 \left(n f_0\right)^2\right)} \tag{2b}$$

where m_d is the adsorbed mass surface density, n is the overtone number, f_0 is the fundamental oscillation frequency, t_q and ρ_q are, respectively, the thickness and density of the quartz crystal, h_1 is the thickness of the adsorbed layer, η_w and ρ_w are the viscosity and density of the bulk solvent (buffer), and η_1 and μ_1 are the viscosity and elastic modulus of the adsorbed layer. Hereby, we combine equations 2a and 2b into equation 3:

$$\frac{\Delta f}{n} = -\frac{m_d f_0}{t_q \rho_q} + \frac{\pi \eta_1 \left(f_0\right)^2}{\mu_1} \left(n \Delta D\right) \tag{3}$$

which shows that, if the thin film asumption holds, a plot of $\Delta f\, n^{-1}$ vs. $n\Delta D$ at different values of n should be a line with a y-intercept equal to $-(m_d f_0)\,(t_q \rho_q)^{-1}$. This value corresponds to the frequency shift expected from a rigid film with the same mass surface density, as described by the Sauerbrey equation [30]. Notice that the determination of the mass surface density according to the linearization proposed in equation 3 does not require any previous knowledge concerning the film density, shear moduli or viscosity. It is, however, necessary to assume that the thickness of the film is small enough for the limit to be applied. Here we propose that equation 3 may be useful to rapidly fit the data when the immobilized mass is the

only output parameter of interest. All reported values were calculated from equation 3 and the $\Delta f\, n^{-1}$ and $n\Delta D$ values obtained from at least four overtones.

Immobilization of lipodisks on QCM-D sensors

QCM-D gold sensors were cleaned with hot piranha solution (3:1 sulfuric acid:hydrogen peroxide) for 40 s, rinsed with MilliQ water and absolute ethanol, and then incubated overnight in MUA 1 mM in absolute ethanol. Before use, the sensor was rinsed in absolute ethanol for at least 10 min and dried under a gentle nitrogen flow. After mounting of the sensor, the system was equilibrated with MilliQ water until a stable baseline was obtained. The surface was then activated for 10 min with a freshly prepared 0.1 M NHS : 0.4 M EDC 1:1 mixture. After activation, the system was flushed first with 80 mM acetate buffer (pH 4.5) for 10 min followed by PBS until a stable baseline was obtained. A suspension of amine functionalized lipodisks (0.5-1 mM total lipid concentration) in PBS was then loaded and allowed to react at diminished flow rate (0-50 μL/min) until a stable value for the changes in frequency and dissipation was obtained (usually ~2 h). The system was then rinsed with a 150 μL min^{-1} flow of PBS to remove any non-bound lipodisks. The recorded shifts were stable even when the system was left for up to 24 hours under PBS, discarding thus the possibility that the immobilized structures are released during the experiments. The amount of bound lipid was calculated from the dissipation and frequency shifts according to equation 3. Two other lipodisk immobilization protocols were evaluated. Direct binding to gold via thiol chemistry (employing thiol-modified PEG lipids) and binding via streptavidin crosslinking between biotynilated sensor surfaces and biotynilated PEG lipids were tested. However, the immobilization via amine coupling provided with more stable QCM-D signals and allowed also for the reuse of the sensor surface. All experiments described were therefore performed on lipodisks immobilized by this latter method.

Interaction of alpha-helical amphiphilic peptides with immobilized lipodisks

Association isotherms of melittin, mastoparan, and mastoparan X with the lipodisks were determined according to the following protocol. After disk immobilization, the remaining active surface was inactivated by a 10 min flow of 1 M ethanolamine hydrochloride at pH = 8.5. After the inactivation period, the system was equilibrated with the working buffer (PBS). In order to determine the peptide-disk binding isotherms, solutions with increasing concentrations of the corresponding peptide were sequentially loaded into the system. In order to account for the "bulk effect", i.e., the shifts arising from changes in density and viscosity of the bulk solution, frequency and dissipation displacements caused only by bulk effects were recorded on an inactive sensor. This allowed substracting the changes caused by the bulk effect from the peptide binding signals, in agreement with previous reports[31]. Complementarily, the system was rinsed with the working buffer after equilibration with each peptide concentration. This opens the possibility of studying the peptide release process. Furthermore, if the analyte is irreversible bound, this treatment allows quantitative determinations without the need of independently determining the bulk effect. However, in the present case, it is likely that such treatment would cause the release of the peptides and therefore the bulk effect substraction was the preferred approach for quantitative determinations. Knowing the amount of bound lipid and associated peptide, isotherms to describe the interaction were generated. The R_{eff} values at different peptide concentrations were calculated from the obtained data.

Results and discussion

Covalent coupling of disks to QCM-D sensor surfaces

Extruded lipodisks could be successfully immobilized on the modified gold sensors via amine coupling by using the protocol described above. Figure 1a shows the QCM-D signal recorded during the immobilization of extruded lipodisks composed of DPPC: DSPE-

PEG_{2000}: DSPE-PEG_{2000}amine 75:21:4. As a relative measurement of the immobilized disks layer rigidity, the $\Delta f/\Delta D$ ratio of the formed layers was determined. For the lipodisks employed in this study, the value is equal to 4.2 ± 0.19 (10^6 Hz) as determined from four repetitions of the immobilization experiment. For comparison, lipodisks prepared by the detergent depletion method, usually much smaller than their extruded counterparts, were also immobilized (Cryo-TEM pictures and DLS data for both lipodisk preparations can be found in Figure S-1 in the Supporting Information). The corresponding $\Delta f/\Delta D$ ratio is 8.54 ± 0.5 (10^6 Hz), from three repetitions, suggesting that the layer formed by the smaller disks is more rigid, and/or that it has a larger intrinsic viscosity due to a smaller size of the immobilized objects, as demonstrated previously[32]. Both interpretations suggest that the lipodisks are arranged perpendicularly to the substrate. Figure 1b shows that the linearization described in equation 3 corresponds well with the obtained experimental data. The maximum obtained amount of immobilized extruded lipodisks was 2600 ng cm^{-2}, corresponding well to the expected thickness of the immobilized layer (~ 24 nm, twice the hydrodynamic radius of the disks) if its density is assumed to be close to that of pure water (1 g cm^{-3}). Furthermore, a rough theoretical value of the expected immobilized mass when a tightly packed lipodisk layer is formed was estimated. This calculation considered the average size distribution of the lipodisk suspensions and the average density of the lipid mixture used. It is, however, necessary to remark that several assumptions need to be made. First, the size distribution obtained by DLS needs to be corrected to obtain the radius of the disks (R_{Disk}) according to Mazer et al.[33]:

$$R_{\mathrm{H}} = \frac{3R_{\mathrm{Disk}}}{2}\left\{\left(1+\alpha^2\right)^{1/2} + \left(\frac{1}{\alpha}\right)\ln\left(\alpha+\left(1+\alpha^2\right)^{1/2}\right) - \alpha\right\}^{-1} \qquad (4)$$

where R_{H} is the hydrodynamic radius determined by DLS (shown in Figure S-1 in the Supporting Information), and α is given by $L_{\mathrm{Disk}}/(2R_{\mathrm{Disk}})$, where L_{Disk} is the thickness of the

lipodisks. The latter was estimated as 11.7 nm, according to the data reported by Johnson et al.[34] Secondly, the mean density of the lipodisks (ρ_{Disk}) was determined from:

$$\rho_{\text{Disk}} = x_{\text{DPPC}}\left(\frac{M_{\text{w(DPPC)}}}{N_{\text{A}}A_{\text{DPPC}}L_{\text{DPPC}}}\right) + x_{\text{DSPE-PEG2000}}\left(\frac{M_{\text{w(DSPE-PEG2000)}}}{N_{\text{A}}A_{\text{DSPE}}L_{\text{DSPE}} + \left(2000/\rho_{\text{PEG2000}}\right)}\right) \qquad (5)$$

where $x_{\text{DPPC}} = 0.75$ and $x_{\text{DSPE-PEG2000}} = 0.25$ represent the molar fractions of the indicated components, $M_{\text{w(DPPC)}} = 734\ \text{g mol}^{-1}$ and $M_{\text{w(DSPE-PEG2000)}} = 2805.54\ \text{g mol}^{-1}$ are the respective molecular weights, $A_{\text{DPPC}} = 47.9\ \text{Å}^2$, $A_{\text{DSPE}} = 43\ \text{Å}^2$ and $L_{\text{DPPC}} = 2.2\ \text{nm}$, $L_{\text{DSPE}} = 2.35\ \text{nm}$ are the literature values[35,36] for the cross sectional area (A) and length (L) of the indicated molecules, N_{A} is the Avogadro constant, and $\rho_{\text{PEG2000}} = 1210\ \text{kg m}^{-3}$ is the density of bulk PEG2000. The value thus calculated is $\rho_{\text{Disk}} = 1185.2\ \text{kg m}^{-3}$. Using this value and the R_{Disk} distribution calculated from equation 4, the average surface mass density on the sensor for a tightly packed lipodisk layer was estimated. to be ~3550 ng cm^{-2}, suggesting that in our experiments only about 75% surface coverage can be obtained. This incomplete coverage can be easily understood, as the coupling reaction with the sensor should be occurring at random points on the surface, not allowing for optimal conformation of the disks to achieve full coverage. The relatively loose packing of the immobilized disks makes it plausible to assume that the whole area of the lipodisks is available for interactions with analytes in the bulk solution.

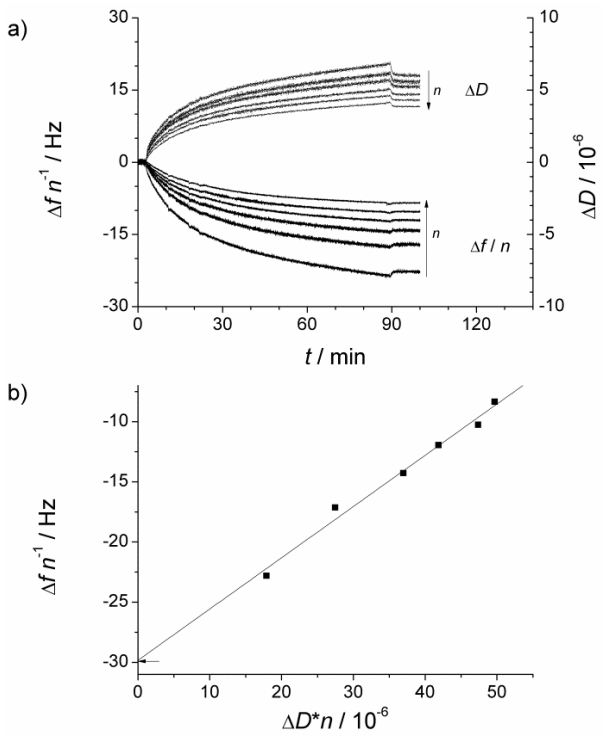

Figure 1. a) Shifts in frequency and dissipation obtained during a QCM-D experiment. Data obtained upon immobilization of extruded DPPC:DSPE-PEG_{2000} lipodisks (loading lipodisk concentration = 750 μM) via amine coupling on activated gold sensors. The arrows indicate increasing overtone number n = 3, 5, 7, 9, 11 and 13 b) Linearization according to equation 3. The data plotted is calculated from the last experimental point shown in (a). The arrow indicates the y-intercept, equivalent to the frequency shift expected from a rigid film with the same mass. Fitting parameters: Slope = 0.426 ± 0.025 (10^6 Hz), y-intercept = -29.83 ± 0.96 Hz.

The mass data obtained from equation 3 was compared with the results from the fitting with the standard QTools software for anlaysis of QCM-D data. This approach requires previous knowledge of at least one of the layer properties represented in equations 2a and 2b. In this case, the density of the formed layer was assumed to be the same as for water: 1000 kg m^{-3}. The QTools fitting had the great disadvantage that, for the same set of data, it would report different values when the parameter fitting range was modified. The lowest chi-square value was usually obtained together with an estimated immobilized mass which was clearly

overestimated (up to 10000 ng cm^{-2}, corresponding to a layer thickness of 100 nm, more than 4 times the 24 nm hydrodynamic diameter determined by DLS and exceeding the mass expected from tight packing of the immobilized lipodisks). Limiting the fitting parameters, more reliable mass densities were obtained, even though the chi-square value increased significantly. The surface mass densities determined in this way were slightly larger (~15% difference) than those obtained using equation 3. These differences arise most likely from how the data is weighted in the different approaches.

In order to independently test the accuracy of the QCM-D determination of the amount of immobilized lipid, lipodisks labeled with 2 mol-% of DPH were prepared and immobilized on the sensors. DPH was incorporated into the disks by heating the disks suspension to 60 °C and adding the desired DPH amount from a stock solution in methanol. The system was then let to equilibrate for 1 h and the disks were immobilized according to the same protocol as for non-labeled disks. After immobilization of the lipodisks, the sensor was carefully dismounted while keeping it wet, and placed in a clean vial. 600 µL of a 0.8 mM $C_{12}E_8$ solution in PBS were then added to dissolve the bound disks. The lipid concentration in the resulting solution was determined by fluorescence spectroscopy from the DPH emission at 425 nm at an excitation wavelength of 365 nm. The standard addition approach was employed. The emission intensity was measured first for the pure sample. Then, five additions (1 µL each) of a concentrated standard solution were performed. The emission intensity was recorded after each addition. The standard used was prepared from labeled lipodisks dissolved in the same detergent solution as the sample to be analized. Plotting the measured emission intensity against the concentration of added standard a straight line is obtained. Extrapolating the line to find the x-intercept allows calculating the concentration of the original sample. The estimated amount of total lipid in the solution was in very good agreement (less than 10% difference) with what was calculated from the evaluation of the QCM-D data according to

equation 3. As an example, Figure 2 shows the standard addition curve for the determination of the concentration of lipid in a solution produced from an immobilized labeled lipodisks layer. The results show that the QCM-D determinations of the immobilized mass are accurate and provide trustworthy values allowing for quantitative interaction studies.

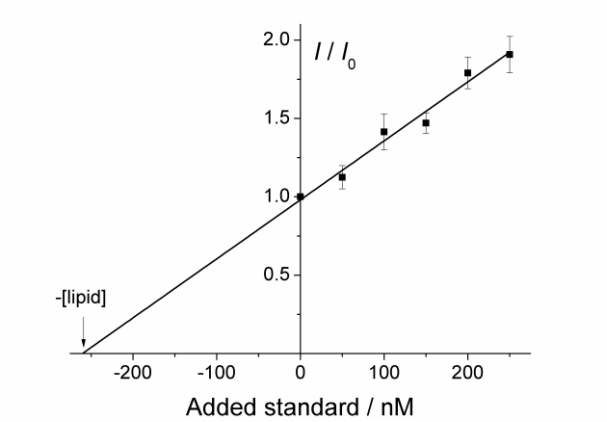

Figure 2. Standard addition curve obtained from the dissolution of 190 ng cm^{-2} immobilized lipodisks on a QCM-D sensor. I/I_0 represents the normalized fluorescence intensity (intensity I after standard addition divided by the intensity of the pure sample I_0). The expected lipid concentration is 241 nM. The calculated lipid concentration ([lipid]) is 260 nM. The linearity of the fluorescence response between 50 and 650 nM lipid was confirmed in a separate experiment. Error bars are given by the standard deviation from three repetitions using different aliquotes.

Characterization of the peptide-lipodisk interaction

The association of alpha-helical amphiphilic peptides with immobilized extruded lipodisks was characterized as described in the methods section. The sequential increments in the loaded peptide concentration lead to a stepwise drop of the recorded oscillation frequency as is exemplified in Figure 2 for the case of mastoparan X. The dissipation factor, on the other hand, changes only marginally, suggesting that the increase in mass due to the association of the peptides is not coupled with any significant structural changes in the immobilized disks. The rinsing steps caused release of the bound mastoparan X, indicating that the association is

reversible. The release of the peptide is rather slow, as the recorded traces do not return to zero during the time-frame of the experiment. To obtain an accurate approximation of the amount of peptide bound before the rinsing step, frequency and dissipation displacements caused only by bulk effects were substracted from the curve, thus estimating the contribution of peptide binding to the overall signal. Noteworthy, the experiments performed to determine the contribution of bulk effects also showed that no significant binding of the peptide to the inactive sensor surface occurs. For example, after loading a 10 µM mastoparan X solution on an inactivated sensor for 8 min, followed by 10 min rinsing, the change in frequency was merely 0.01 Hz, which is within the noise level of the signal.

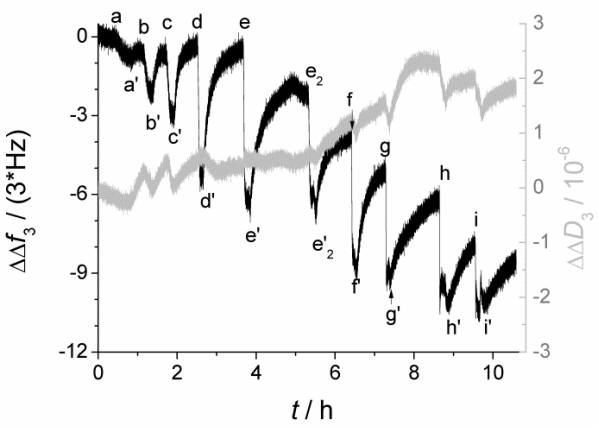

Figure 3. QCM-D data (3rd overtone) showing the binding of mastoparan X to extruded DPPC:DSPE-PEG2000 lipodisks. The labels indicate the addition points of mastoparan X solutions with different concentrations and the corresponding rinsing steps (indicated by an apostrophe). Peptide concentrations: a=0.025 µM; b=0.05 µM; c=0.1 µM; d=0.25 µM; e and e_2=0.5 µM; f=1 µM; g=2.5 µM; h=5 µM, and i=10 µM. A time lapse of 15 h with no buffer flow between e' an e_2 has been omitted.

From the data obtained, the association isotherm of mastoparan X with the lipodisks was determined. Remarkably, the calculated isotherm is very similar to the corresponding curve obtained from well established fluorescence-based methods, as shown in Figure 3. Some differences can be observed, however. For instance, fluorescence and QCM-D measurements

disagree on the peptide binding at low peptide concentrations. Both approaches are based on a range of assumptions that may bias the data and it would therefore be risky to state that the data presented by one of the techniques is more accurate than the other. On the other hand, both techniques predict a similar effective associated peptide to lipid ratio (R_{eff}) at saturation and both agree that at bulk concentrations above ~1 μM the amount of bound peptide increases only marginally with increasing concentration. These are important parameters to consider when designing the loading of lipodisks with amphiphilic peptides for any application and it can therefore be stated that the QCM-D approach can be used with the same confidence level as the fluorimetric determinations.

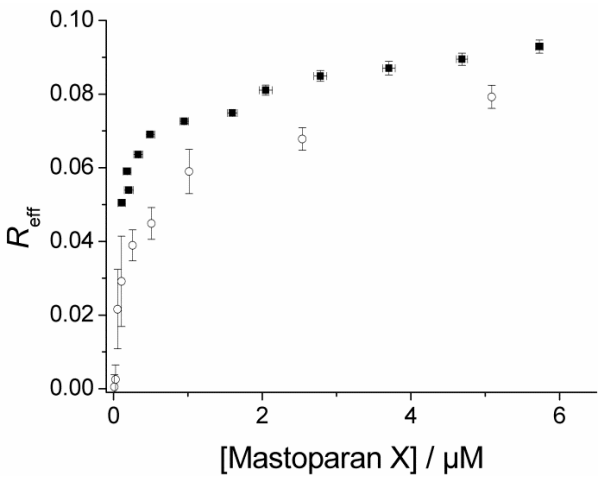

Figure 4. Mastoparan X-lipodisks association isotherm. Filled squares represent the data obtained from fluorimetric determinations. Open circles were obtained from analysis of the QCM-D data. The error bars are given by the standard error calculated from three repetitions in the case of fluorimetric experiments and two repetitions for the QCM-D experiments

Similar experiments as those performed with mastoparan X were carried out using melittin, another alpha-helical amphiphilic peptide presenting intrinsic fluorescence. In contrast to the case with mastoparan X, the QCM-D method did not allow determining the maximum possible amount of bound peptide with accuracy. As can be observed in Figure 4, the QCM-D data is rather scattered. This is completely contrary to what happens with mastoparan X,

where the variance is very small. Notably, the error increases at larger peptide concentrations, where the signals are larger and should therefore be more reliable. Data at higher melittin concentrations than those shown in the figure presented an even larger scattering and are therefore trivial. The reasons for this irreproducibility may lie in the nature of the melittin-lipodisks interaction. Competitive binding assays were performed with lipodisks loaded with melittin and liposomes made of POPC:POPG 90:10 mol:mol and filled with a concentrated solution of CF, a self-quenching dye. The promptness of melittin to detach from the lipodisks and bind to the liposomes was tested by monitoring the CF leakage from the liposomes after addition of lipodisks saturated with the peptide. Figure S-2 in the Supporting Information shows how the leakage from the liposomes is enhanced upon addition of the peptide-lipodisk mixture. It is also shown that a fresh melittin-lipodisk mixture has a more pronounced effect than a matured mixture (24 hours incubation time). This indicates that the detachment of melittin from the disks becomes more difficult over time. Furthermore, when incubating the QCM-D immobilized disks overnight with a melittin solution, the release of the peptide upon rinsing was significantly decreased (Figure S-3, Supporting Information), in agreement with the results from the competitive binding assays. It has recently been recently reported that melittin can react with lipids in the membrane and become acylated[37,38]. The time window in which this reaction occurs for phosphocoline lipids is similar to that in which the affinity changes illustrated in Figures S-2 and S-3 occur, suggesting a possible conection between these observations. Another possible explanation for the apparent time-dependent affinity is the competition between melittin insertion into the membrane and its binding parallel to the membrane surface, a phenomenon that has been described previously[39]. Acylation and conformation competition may, either alone or in concert, account for the large scattering of the melittin-lipodisk binding data in Figure 4. The observation of affinity changes over time would not have been possible with fluorescence measurements, as these provide information

only about the amount of peptide bound to the disks, and not about the reversibility of this interaction. The QCM-D response, on the other hand, is capable of identifying reversible binding upon rinsing. This provides with complementary information concerning the nature of the lipodisk-peptide interaction, which is not available from fluorimetric determinations.

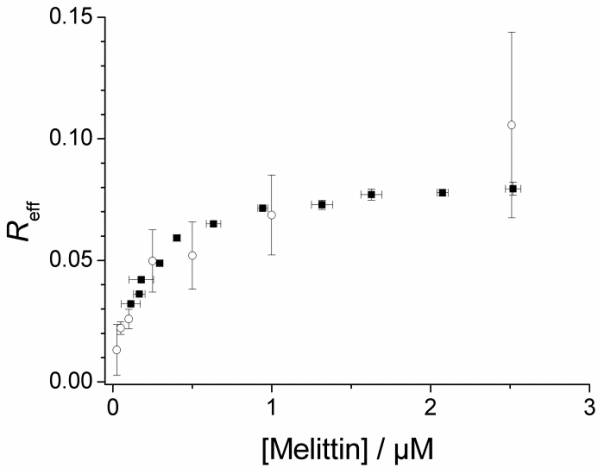

Figure 5. Melittin-lipodisks association isotherm. Filled squares represent the data obtained from fluorimetric determinations. Open circles were obtained from analysis of the QCM-D data. The error bars are given by the standard error calculated from three repetitions of the experiments.

In order to extract quantitative meaningful data from the plots shown in Figures 3 and 4, the association isotherms were analyzed using an association model based on the one proposed for peptide-lipid interactions by Pérez-Paya et al.[40]. This model is given by $R_{eff} = [P]*K/ \gamma_P^{lip}$, where γ_P^{lip} is an activity coefficient to account for deviations from the ideal partition behavior. Wessman et al. [41] defined this coefficient as $\gamma_P^{lip} = \exp(w \times R_{eff})$, where w accounts for electrostatic interactions and for changes in the mechanical properties of the substrate due to peptide binding. In order to get further insight into the possible binding mechanisms, a Scatchard plot ($R_{eff}/[P]$ as a function of R_{eff}) was generated. As shown in Figure 5, the obtained curve is not linear, and it is therefore very unlikely that the peptide-lipodisk

association follows an ideal Langmuir behavior. The non-linearity of the scatchard plot in Figure 5 could arise from the deviations from ideal behavior described by the Pérez-Paya model, or could be independently interpreted as arising from the binding of the peptide to at least two different binding sites (a bi-Langmuir approach): one in which the peptide-disks association is strong and one in which it is much weaker. In principle, and based on previous reported results [42], one can assume that these different sites may represent the lipodisk edges (high affinity for the peptides) and the lipodisk flat faces (lower affinity). Given these properties of the lipodisk as well as the properties of the peptides studied (amphiphilic and positively charged), it is likely that both the bi-Langmuir and the Pérez-Paya models contribute to the final response. Under this assumption, the mixed effects of peptide-peptide repulsion and structural changes, as well as the presence of two different kinds of binding sites would be responsible for the obtained response. In order to obtain quantitative data describing the lipodisk-peptide association, the data was fitted independently to the two models. For the Pérez-Paya model, a plot of $\ln([P]/R_{eff})$ vs. R_{eff} should result in a linear curve with the slope given by w and the y-intercept given by $-\ln(K)$. As exemplified in Figure 5, the model fits very well to the experimental data. In the case of the bi-Langmuir isotherm, only trivial values are obtained for the affinity constants and number of binding sites, as the curve fitting involves a large number (four) of free fitting paramaters. Two of these parameters do not pass the significance test, probably because of the limited number of experimental points. Disregarding these parameters, one ends up with a simple Langmuir model. Even though it is clear that Langmuir behavior is unlikely, fitting to the Langmuir equation provides with meaningful apparent association constants and saturation conditions that facilitate comparisons between peptides. Table 1 shows the calculated peptide-lipodisks association parameters for melittin and mastoparan X according to the model based on the Pérez-Paya isotherm and from the Langmuir isotherm. It is observed that there is good agreement

between the data obtained from fluorimetric determinations and from QCM-D experiments. The only exception is perhaps found for the mastoparan X data fitted with the Pérez-Paya model. However, for this case, the error margins determined for all parameters are rather large. It is therefore likely that the difference in the values reported arises from deviations from the fitting model rather than from discrepancies between the experimental methods. The association parameters of lipodisks and mastoparan (which, contrary to mastoparan X and melittin, has no fluorescent residues) are also shown to illustrate the main advantage of the QCM-D method, i.e., that it can be used even with peptides in which no fluorescent aminoacid or marker is present. The large difference betweeen the association parameters of mastoparan and mastoparan X is also an indication of potentially different behaviors of peptides with similar primary structures. Such changes in membrane-peptide interaction upon modification of the aminoacid sequence have been previously observed in supported bilayer membranes[4]. The present report offers a quantitative description of these changes for the particular case explored. At this point, it is only possible to speculate about the reasons behind this difference, but it is, however, possible to establish that the QCM-D approach can be useful in exploring this and similar issues.

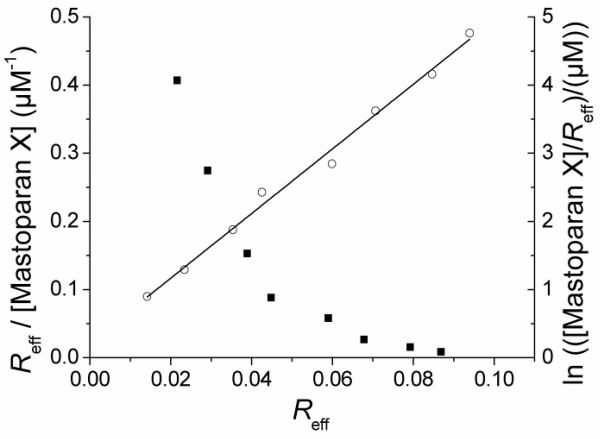

Figure 6. Scatchard plot (left axis, solid squares) and linearization of the Pérez-Paya model (right axis, empty circles. Solid line is given by the linear fitting of the data) obtained for the

association of mastoparan X and extruded lipodisks determined with the QCM-D. Experimental data correspond to what is shown in Figure 3.

Table 1. Parameters describing the association of alpha-helical amphiphilic peptides with DPPC-based extruded lipodisks and comparison of the data obtained from QCM-D and fluorimetric measurements.

Peptide	**Method**	**Langmuir model**[a]		**Pérez-Paya model**	
		K * µM	$R_{eff(max)}$	K * µM	w
Mastoparan X	QCM-D	2.3 ± 0.4	0.089 ± 0.002	2.1 ± 1.3	57.8 ± 11
	Fluorescence	1.8 ± 0.5	0.092 ± 0.006	0.21 ± 0.23	25.3 ± 15
Melittin	QCM-D	6.0 ± 2	0.095± 0.028	1.65 ± 0.77	45.1 ± 13
	Fluorescence	4.3 ± 0.4	0.089 ± 0.001	1.46 ± 0.34	45.3 ± 3.6
Mastoparan	QCM-D	12.9 ± 3.2	0.27 ± 0.003	14.5 ± 6.4	18.0 ± 2.3

[a] Calculated from the Langmuir linearization. Apparent values.

Kinetic studies

Besides the determination of peptide-lipodisks affinity parameters, the time resolution provided by the QCM-D instrument allows following the kinetics of the peptide binding and detachment processes if their time constants are in the magnitude of a few minutes and if they last longer than the equilibration of the signal due to bulk effects. In the present case, only the binding of mastoparan X fulfills these conditions. From the experimental data and equation 3, the amount of bound peptide as a function of time can be determined. The binding kinetics can then be studied. Furthermore, giving that the peptide is released during the rinsing steps, the detachment kinetics can also be studied. The easiest and more direct approach is to fit the binding and detachment as functions of time to a single exponential decay equation ($MPX_{disks}=A_0 + A_1*\exp(-t/\tau_1)$, where MPX_{Disks} represents the amount of mastoparan X bound to the disks, τ_1 is the time constant of the process and A_i are fitting parameters related to the

initial and saturation conditions of the experiment), assuming thus first or pseudo-first order kinetics. As shown in Figure 6, a good agreement with the experiment is obtained. It is necessary to remark that the used kinetic equation is merely empirical and that the obtained parameters apply only for a certain mastoparan X concentration. Particularly, the time constant changes significantly when the concentration is modified, as is expected for pseudo-first order kinetics. Determining the binding affinity from the kinetic data is therefore not reliable, although it may in principle provide a qualitative approximation when comparing different peptides. Although a formal kinetic model is lacking, the simple exponential equation proposed provides kinetic parameters to describe the process under specific conditions, which can be useful to predict the binding and release behavior of the peptide under circumstances of interest (e.g., how fast the peptide would be released from the disk under physiological conditions).

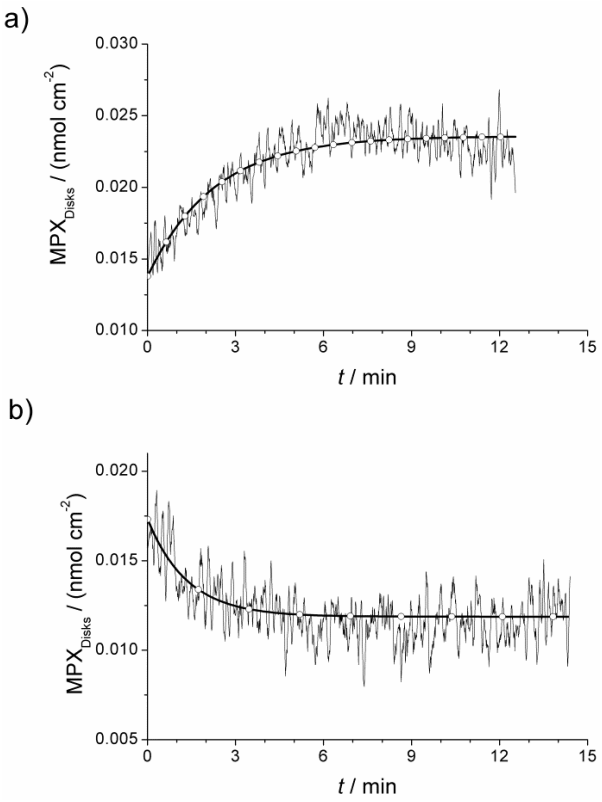

Figure 7. a) Binding of mastoparan X to lipodisks from a 0.05 μM peptide solution (τ_1 = 136 s) and b) detachment of the peptide upon rinsing (τ_1 = 81 s). MPX_{Disks} was calculated from

the QCM-D data presented in Figure 2 and equation 3. Thicker curves are given by fitting the data to an exponential decay equation.

Conclusions

The results reported in this study illustrate the analytical potential of immobilized lipodisks. In addition to previously reported interaction parameters of proteins and lipodisks [5,27], the characterization of the affinity between lipodisks and low molecular weight peptides opens the possibility of studying the membrane interaction of smaller molecules. It represents also a big step towards the characterization of the binding of anti-microbial peptides of therapeutical relevance to potential delivery vehicles such as the lipodisks. The fact that both thermodynamic and kinetic parameters can be available may allow for an optimal design of the lipodisks before they are tested as drug carriers under specific conditions. As non-fluorescent peptides can be studied, the range of application is much wider than that of established fluorimetric methods, while the results obtained have a similar level of confidence. Furthermore, the modification of the peptides with fluorescent residues that may significantly affect the binding behavior (as illustrated in this report) is avoided, and the peptides can therefore be studied in their native state.

Future work carried out with the method here described may fully characterize the parameters that control the peptide-lipodisk interaction, such as nature of the peptide, composition and size of the lipodisks, composition and charge of the lipodisk rim, ionic strenght of the bulk solution, etc. It should then be possible to characterize the nature of the binding sites and to elucidate a better association isotherm that takes into account the differences between binding to the lipodisks rim or planar surfaces, peptide-peptide interactions, and even changes on the nature of the binding sites upon peptide adsorption.

Supporting information

Supporting information available:

Figure S-1: Cryo-TEM and DLS images and data, respectively, obtained for DPPC: DSPE-PEG_{2000}: DSPE-PEG_{2000}amine 75:21:4 lipodisks prepared by extrusion and detergent depletion.

Figure S-2: CF leakage from POPC:POPG 90:10 liposomes after addition of a fresh (less than 2 h incubation time) and of a matured (between 24-26 h incubation time) melittin-lipodisk mixture.

Figure S-3: QCM-D signals obtained for the rinsing of lipodisks equilibrated with 2.5 µM melittin during 8 min and during 17 h.

This material is available free of charge via the Internet at http://pubs.acs.org.

Acknowledgments

We thank Dr. Jonny Eriksson for technical assistance with the Cryo-TEM analysis. Financial support from the Swedish cancer Society and the Swedish Research Council is gratefully acknowledged.

References

(1) Burgess, I.; Li, M.; Horswell, S. L.; Szymanski, G.; Lipkowski, J.; Majewski, J.; Satija, S. *Biophys. J.* **2004**, *86*, 1763-1776.

(2) Nelson, A. *Curr. Opin. Colloid Interface Sci.* **2010**, *15*, 455-466.

(3) Du, L.; Liu, X.; Huang, W.; Wang, E. *Electrochim. Acta* **2006**, *51*, 5754-5760.

(4) McCubbin, G. A.; Praporski, S.; Piantavigna, S.; Knappe, D.; Hoffmann, R.; Bowie, J. H.; Separovic, F.; Martin, L. L. *Eur. Biophys. J. Biophy.* **2011**, *40*, 437-446.

(5) Vainikka, K.; Reijmar, K.; Yohannes, G.; Samuelsson, J.; Edwards, K.; Jussila, M.; Riekkola, M.-L. *Anal. Biochem.* **2011**, *414*, 117-124.

(6) Jung, H.; Robison, A. D.; Cremer, P. S. *J. Struct. Biol.* **2009**, *168*, 90-94.

(7) Terrettaz, S.; Vogel, H. *Mrs Bulletin* **2005**, *30*, 207-210.

(8) Gordillo, G. J.; Schiffrin, D. J. *Faraday Discuss.* **2000**, *116*, 89-107.

(9) Moncelli, M. R.; Herrero, R.; Becucci, L.; Guidelli, R. *Biochim. Biophys. Acta* **1998**, *1364*, 373-384.

(10) Mårtensson, C.; Agmo Hernández, V. *Bioelectrochemistry* **2012**, *88*, 171-180.

(11) Yao, W. W.; Lau, C.; Hui, Y. L.; Poh, H. L.; Webster, R. D. *J. Phys. Chem. C* **2011**, *115*, 2100-2113.

(12) Hosseini, A.; Collman, J. P.; Devadoss, A.; Williams, G. Y.; Barile, C. J.; Eberspacher, T. A. *Langmuir* **2010**, *26*, 17674.

(13) Correia-Ledo, D.; Arnold, A. A.; Mauzeroll, J. *J. Am. Chem. Soc.* **2010**, *132*, 15120-15123.

(14) Largueze, J.-B.; El Kirat, K.; Morandat, S. *Colloid. Surface. B* **2010**, *79*, 33-40.

(15) Castellana, E. T.; Cremer, P. S. *Surf. Sci. Rep.* **2006**, *61*, 429-444.

(16) Borch, J.; Torta, F.; Sligar, S. G.; Roepstorff, P. *Anal. Chem.* **2008**, *80*, 6245-6252.

(17) Wadsater, M.; Laursen, T.; Singha, A.; Hatzakis, N. S.; Stamou, D.; Barker, R.; Mortensen, K.; Feidenhans'l, R.; Moller, B. L.; Cardenas, M. *J. Biol. Chem.* **2012**, *287*, 34596-34603.

(18) Sloan, C. D. K.; Marty, M. T.; Sligar, S. G.; Bailey, R. C. *Anal. Chem.* **2013**, *85*, 2970-2976.

(19) Tark, S.; Das, A.; Sligar, S.; and Dravid, V. P. *Nanotechnology* **2010**, *21*, 435502.

(20) Denisov, I. G.; Grinkova, Y. V.; Lazarides, A. A.; Sligar, S. G. *J. Am. Chem. Soc.* **2004**, *126*, 3477-3487.

(21) Edwards, K.; Johnsson, M.; Karlsson, G.; Silvander, M. *Biophys. J.* **1997**, *73*, 258-266.

(22) Johansson, E.; Engvall, C.; Arfvidsson, M.; Lundahl, P.; Edwards, K. *Biophys. Chem.* **2005**, *113*, 183-192.

(23) Johnsson, M.; Edwards, K. *Biophys. J.* **2003**, *85*, 3839-3847.

(24) Zetterberg, M. M.; Reijmar, K.; Pränting, M.; Engström, Å.; Andersson, D. I.; Edwards, K. *J. Control. Release* **2011**, *156*, 323-328.

(25) Lundquist, A.; Hansen, S. B.; Nordström, H.; Danielson, U. H.; Edwards, K. *Anal. Biochem.* **2010**, *405*, 153-159.

(26) Boija, E.; Lundquist, A.; Nilsson, M.; Edwards, K.; Isaksson, R.; Johansson, G. *Electrophoresis* **2008**, *29*, 3377-3383.

(27) Meiby, E.; Morin Zetterberg, M.; Ohlson, S.; Agmo Hernández, V.; Edwards, K. *Anal. Bioanal. Chem.* **2013**, *405*, 4859-4869.

(28) Wessman, P.; Morin, M.; Reijmar, K.; Edwards, K. *J. Colloid Interf. Sci.* **2010**, *346*, 127-135.

(29) Voinova, M. V.; Rodahl, M.; Jonson, M.; Kasemo, B. *Phys. Scripta* **1999**, *59*, 391-396.

(30) Sauerbrey, G. *Z. Phys.* **1959**, *155*, 206-222.

(31) Bordes, R.; Hook, F. *Anal. Chem.* **2010**, *82*, 9116-9121.

(32) Tsortos, A.; Papadakis, G.; Gizeli, E. *Biosens. Bioelectron.* **2008**, *24*, 836-841.

(33) Mazer, N. A.; Benedek, G. B.; Carey, M. C. *Biochemistry-US* **1980**, *19*, 601-615.

(34) Johnsson, M.; Hansson, P.; Edwards, K. *J. Phys. Chem. B* **2001**, *105*, 8420-8430.

(35) Nagle, J. F.; Tristram-Nagle, S. *BBA -Rev. Biomembranes* **2000**, *1469*, 159-195.

(36) Kuhl, T. L.; Leckband, D. E.; Lasic, D. D.; Israelachvili, J. N. *Biophys. J.* **1994**, *66*, 1479-1488.

(37) Dods, R. H.; Mosely, J. A.; Sanderson, J. M. *Org. Biomol. Chem.* **2012**, *10*, 5371-5378.

(38) Pridmore, C. J.; Mosely, J. A.; Rodger, A.; Sanderson, J. M. *Chem. Commun.* **2011**, *47*, 1422-1424.

(39) van den Bogaart, G.; Guzman, J. V.; Mika, J. T.; Poolman, B. *J. Biol. Chem.* **2008**, *283*, 33854-33857.

(40) PerezPaya, E.; Porcar, I.; Gomez, C. M.; Pedros, J.; Campos, A.; Abad, C. *Biopolymers* **1997**, *42*, 169-181.

(41) Wessman, P.; Stromstedt, A. A.; Malmsten, M.; Edwards, K. *Biophys. J.* **2008**, *95*, 4324-4336.

(42) Lundquist, A.; Wessman, P.; Rennie, A. R.; Edwards, K. *BBA-Biomembranes* **2008**, *1778*, 2210-2216.

For TOC only